

Equivalent Circuit Based Non-linear Microwave Model for FinFETs

G. Crupi^{*}, D. M. M.-P. Schreurs^{**}, I. Angelov^{***}, A. Caddemi^{****}, and B. Parvais^{*****}

^{*}DFMTFA, University of Messina, 98166 Messina, ITALY.
Electronic Engineering Department, K.U.Leuven, B-3001 Leuven, BELGIUM.
Phone: +39-0903977375; Fax: +39-090391382; E-mail: giocrupi@ingegneria.unime.it

^{**}Electronic Engineering Department, K.U.Leuven, B-3001 Leuven, BELGIUM.
E-mail: Dominique.Schreurs@esat.kuleuven.be

^{***}Microwave Electronic Laboratory, Department of Microtechnology and Nanoscience,
Chalmers University of Technology, SE-41296 Göteborg, SWEDEN.
E-mail: iltcho@chalmers.se

^{****}DFMTFA, University of Messina, 98166 Messina, ITALY.
E-mail: caddemi@ingegneria.unime.it

^{*****}IMEC, B-3001 Leuven, BELGIUM.
E-mail: parvais@imec.be

Abstract-Equivalent circuit based non-linear microwave modelling is studied for the case of FinFET devices. Firstly, an accurate multi-bias small signal equivalent circuit is extracted and then used for building a non-linear full blown lookup table model. Subsequently, an alternative model implementation, which is based on empirical functions, has been investigated. A fully validation of the extracted non-linear models is achieved by comparing their simulation results with large signal measurements.

Index Terms- Angelov model, FinFET, large signal measurements, lookup table model.

I. INTRODUCTION

Over the last decade, the FinFET is emerging as promising multiple gate MOSFET structure to extend the limit of the channel length downscaling into the nanometer regime [1-3]. Accurate and robust non-linear microwave modelling of this emerging transistor is an essential step for an efficient development of the fabrication and design processes. In order to accomplish this task, we begin with an analytical extraction of the extrinsic small signal equivalent circuit parameters (ECPs), which are assumed bias independent. These extrinsic linear elements are at the heart of a successful non-linear model, because their effects have to be removed from the

measurements before determining the intrinsic non-linear circuit. Next we calculate the intrinsic ECPs at each bias point and their bias dependence is used for analytically building a non-linear lookup table model [3]. Additionally, we also represent the intrinsic non-linear circuit by using empirical functions [4, 5], which are determined with optimization and tuning procedures. As it will be shown, both non-linear modelling approaches lead to accurate and robust models, which are fully validated through the comparison between simulations and large signal network analyzer (LSNA) measurements at different bias points, fundamental frequencies, and input powers. Note that empirical models (EMs), especially the default models, are with fixed configuration and will not reproduce accurately strange effects or bias dependencies (or will not be accurate). In such a cases EM will require very complex modelling functions, which can be difficult to create and fit. From this point of view, the table based approach can be very accurate, but extraction can be complicated for large, high power and/or high frequency devices. I.e., depending on the case, we should switch to the right modelling approach. For technology settled process and standard device characteristics, it can be reasonable to use the EMs since they are easy to understand and extract using the CAD tool directly. Important benefit is that EM can be

used in bias conditions and frequency far from the measurement range, i.e., extrapolations works very well for the EM. And the best is to combine both approaches.

II. NON-LINEAR MODEL EXTRACTION

The investigated device, which is fabricated in FinFET technology [2], has a gate length of 60 nm and a total gate width of 45.6 μm consisting of 50 fingers covering 6 fins each. Fig. 1 shows the circuit topology used for representing the small signal behaviour of the FinFET, after having applied the two-step de-embedding procedure to the Scattering (S -) parameter measurements [2]. This equivalent circuit consists of six extrinsic elements C_{pg} , C_{pd} , L_g , R_g , R_s , R_d and nine intrinsic elements C_{gs} , R_{gs} , C_{gd} , R_{gd} , g_m , τ , R_{ds} , C_{ds} , R_{sub} . All extrinsic ECPs are analytically obtained from S -parameters at zero drain-source voltage [2]. Subsequently, the intrinsic ECPs are determined at each bias point from the intrinsic admittance (Y -) parameters. The obtained multi-bias small signal model is validated up to 50 GHz and then used as cornerstone for constructing the non-linear quasi-static model (see Fig. 2), which is represented with lookup tables [3]. The quasi-static assumption allows to neglect R_{gs} , R_{gd} , R_{sub} , τ , and is adopted since the fundamental frequency for the non-linear model validation is not higher than 5 GHz. This is due to the wide range of possible applications around this frequency. The gate current source I_{gsi} , which includes both the gate-source and gate-drain currents, is directly measured in DC and stored in the table vs. the intrinsic voltages V_{dsi} and V_{gsi} . The sources I_{dsiRF} and Q_{gs} , Q_{ds} are determined from the integration of g_m , g_{ds} and C_{gs} , C_{gd} , C_{ds} with respect to V_{dsi} and V_{gsi} . Note that in the case of the tested FinFET, the dependence of the integration results on the chosen starting point and path is very small and the I_{dsiRF} values are similar to the corresponding I_{dsiDC} values directly measured in DC (see Fig. 3). However, in order to eliminate this small current difference, we use two output current sources in combination with a capacitance, as reported in Fig. 2, instead of only I_{dsiRF} . This solution leads to simulated DC characteristics identical to the measured ones. As shown, the non-linear lookup table model can be straightforwardly implemented. On the other hand, the non-linear

empirical model requires optimization and/or tuning processes but offers the advantage of being represented by a limited number of parameters. For that reason, we also determine an empirical model (see Fig. 4) which is obtained from the Angelov model available in Advanced Design System [6] by accounting that the self-heating and intrinsic non-quasi static effects can be neglected in the present case. The bias dependence of the intrinsic current sources and capacitances, which are used in place of the charge sources, are described with empirical functions [6]. The function parameters are determined by fitting both DC and LSNA measurements. Fig. 5 shows that the obtained empirical model can successfully reproduce the measured I_{ds} . Note that the gate current sources of both non-linear models represent the gate current obtained from DC measurements. We neglected the associated resistance R_{gsf} and R_{gdf} during the small signal analysis, since the FinFETs are DC insulated gate devices and consequently both resistances are extremely high.

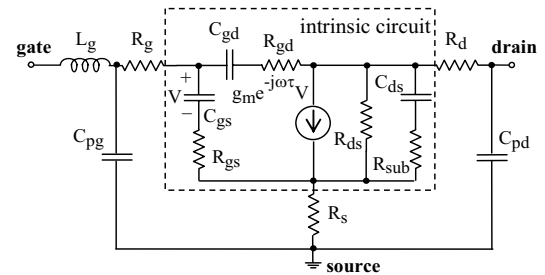


Fig.1. Linear FinFET equivalent circuit.

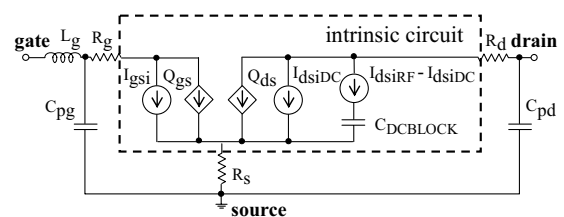


Fig.2. Non-linear FinFET equivalent circuit.

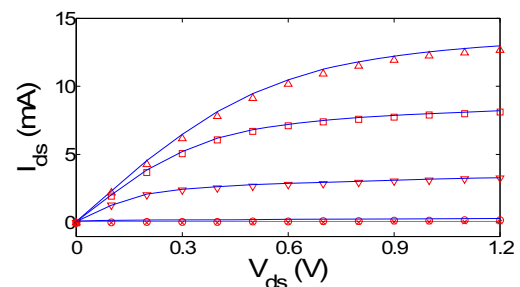


Fig.3. Simulations by the table model based on I_{dsiRF} (lines) and measurements (symbols) of I_{ds} vs. V_{ds} ; V_{gs} is equal to 0, 0.3, 0.6, 0.9, 1.2 V.

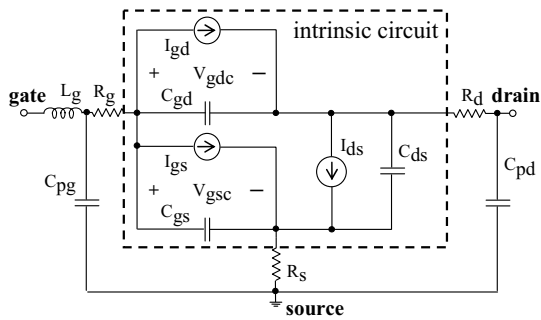
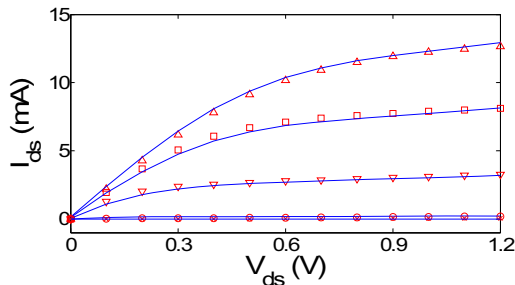


Fig.4. Non-linear FinFET equivalent circuit.


 Fig.5. Empirical model simulations (lines) and measurements (symbols) of I_{ds} vs. V_{ds} ; V_{gs} is equal to 0, 0.3, 0.6, 0.9, 1.2 V.

III. NON-LINEAR MODEL VALIDATION

The extracted non-linear models are fully validated by comparing their simulations with large signal network analyzer measurements. The advantage of using an LSNA set-up is that both amplitude and phase spectra of all travelling voltage waves are measured and hence the non-linear microwave behaviour of the tested device is fully determined [7]. A two-step de-embedding procedure is applied to the LSNA measurements [3], since the non-linear models are based on the multi-bias small signal equivalent circuit, extracted from de-embedded S -parameters. Figs. 6 and 7 highlight that both table based and empirical approaches lead to accurate and robust models that can reproduce successfully the LSNA measurements at different working conditions: input power, bias point, and fundamental frequency. As expected, the nonlinearities decrease at lower input power. As a matter of fact, Figs. 6 (b) and 7 (b) indicate a reduced top and bottom clipping of the I_{ds} waveform, due to the self-biasing effect of the device in the linear and pinch-off regions, and a reduced distortion of the ellipse shape of the input locus.

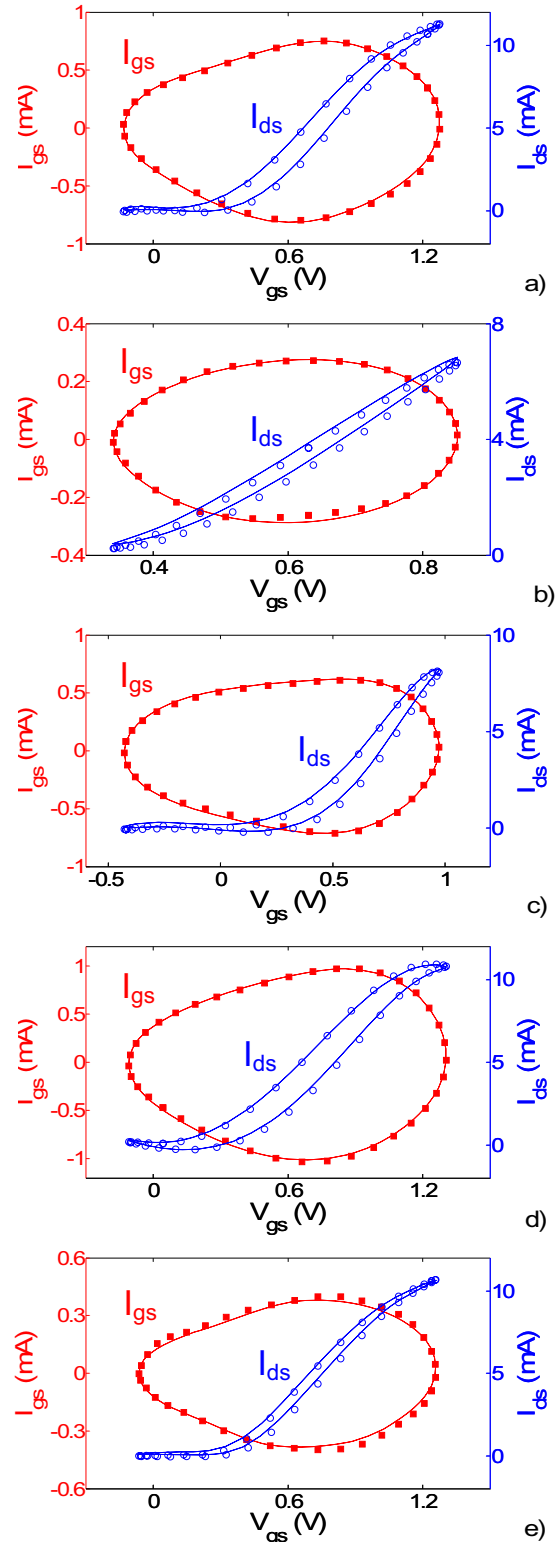


Fig.6. Lookup table model simulated (lines) and measured (symbols) input (left axes) and transfer (right axes) loci of a FinFET at: a) $V_{gs} = 0.6$ V, $V_{ds} = 0.9$ V, $P_{in} = 0.9$ dBm, $f_0 = 4$ GHz, b) $V_{gs} = 0.6$ V, $V_{ds} = 0.9$ V, $P_{in} = -7.8$ dBm, $f_0 = 4$ GHz, c) $V_{gs} = 0.3$ V, $V_{ds} = 0.9$ V, $P_{in} = 0.9$ dBm, $f_0 = 4$ GHz, d) $V_{gs} = 0.6$ V, $V_{ds} = 0.9$ V, $P_{in} = 1.0$ dBm, $f_0 = 5$ GHz, e) $V_{gs} = 0.6$ V, $V_{ds} = 0.9$ V, $P_{in} = 0.4$ dBm, $f_0 = 2$ GHz.

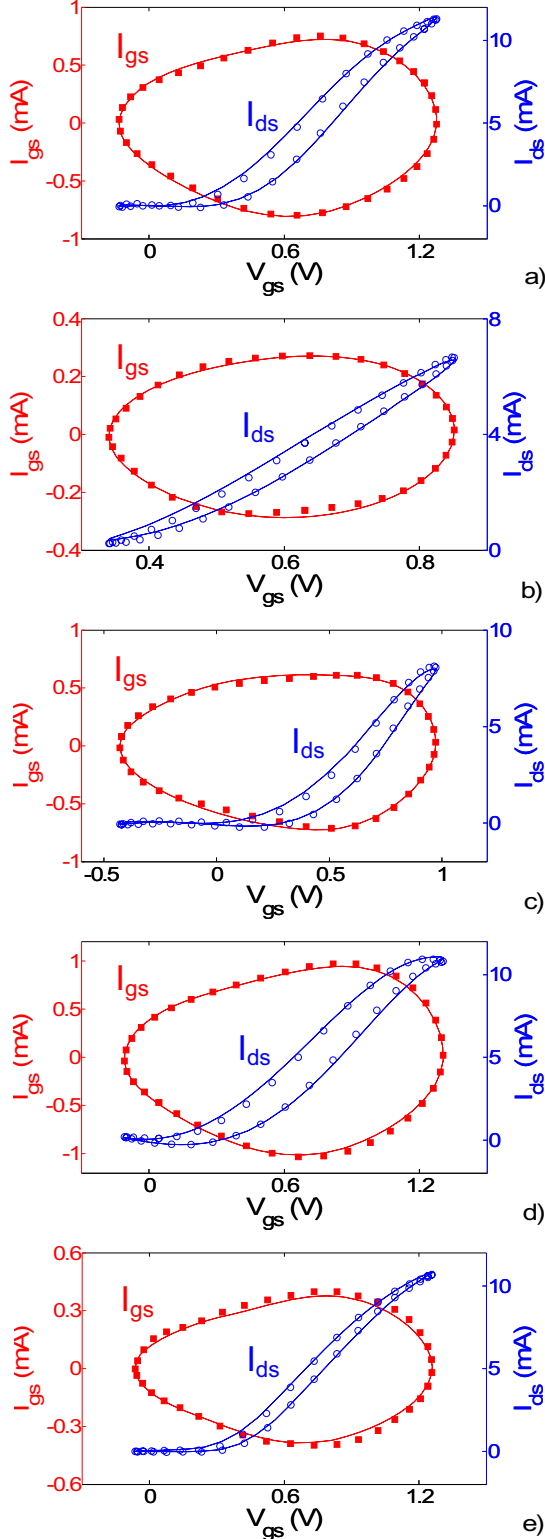


Fig.7. Empirical model simulated (lines) and measured (symbols) input (left axes) and transfer (right axes) loci at: a) $V_{gs} = 0.6$ V, $V_{ds} = 0.9$ V, $P_{in} = 0.9$ dBm, $f_0 = 4$ GHz, b) $V_{gs} = 0.6$ V, $V_{ds} = 0.9$ V, $P_{in} = -7.8$ dBm, $f_0 = 4$ GHz, c) $V_{gs} = 0.3$ V, $V_{ds} = 0.9$ V, $P_{in} = 0.9$ dBm, $f_0 = 4$ GHz, d) $V_{gs} = 0.6$ V, $V_{ds} = 0.9$ V, $P_{in} = 1.0$ dBm, $f_0 = 5$ GHz, e) $V_{gs} = 0.6$ V, $V_{ds} = 0.9$ V, $P_{in} = 0.4$ dBm, $f_0 = 2$ GHz.

VI. CONCLUSION

Both lookup table and empirical approaches have been accurately implemented and successfully validated in the case of FinFET. It has been shown that the former can be easily and analytically implemented, while the latter needs tuning and/or optimization procedures. On the other hand, the empirical approach leads to a more compact representation.

ACKNOWLEDGMENT

The authors would like to thank Dongping Xiao, Dr. Abdelkarim Mercha, and Dr. Stefaan Decoutere for their helpful support. This work was supported by “TARGET” under Contract IST-1-507893-NOE, “Nano-RF” project under Contract IST-027150, and “IMT-ARSEL” project prot. RBIP06R9X5 with financial support by Italian MIUR.

REFERENCES

- [1] V. Subramanian, B. Parvais, J. Borremans, A. Mercha, D. Linten, P. Wambacq, *et al.*, “Planar bulk MOSFETs versus FinFETs: an analog/RF perspective”, *IEEE Trans. Electron Devices*, Vol. 53, pp. 3071-3079, Dec. 2006.
- [2] G. Crupi, D. Schreurs, B. Parvais, A. Caddemi, A. Mercha, and S. Decoutere, “Scalable and multibias high frequency modeling of multi fin FETs”, *Solid-State Electron.*, Vol. 50, pp. 1780-1786, Nov./Dec. 2006.
- [3] G. Crupi, D. Schreurs, D. Xiao, A. Caddemi, B. Parvais, A. Mercha, *et al.*, “Determination and validation of new nonlinear FinFET model based on lookup tables”, *IEEE Microwave and Wireless Comp. Lett.*, Vol. 17, pp. 361-363, May 2007.
- [4] I. Angelov, L. Bengtsson, M. Garcia, “Extensions of the Chalmers Nonlinear HEMT and MESFET model”, *IEEE Trans. Microwave Theory Tech.*, Vol. 44, pp. 1664-674, Oct. 1996.
- [5] I. Angelov, M. Fernhdal, F. Ingvarson, H. Zirath, H. O. Vikes “CMOS large signal model for CAD”, *IEEE MTT-S Digest*, pp. 643-646, June 2003.
- [6] ADS user manual
- [7] J. Verspecht, “Large-signal network analysis”, *IEEE Microwave Magazine*, Vol. 6, pp. 82-92, Dec. 2005.